International Journal of Earthquake Engineering. 2017;34(1):61-81.
http://ingegneriasismica.org/2017/03/.

Stress verifications of large concrete existing dams: comparison of two seismic Italian codes

M. Colombo, DICA, Politecnico di Milano
martina.colombo@polimi.it
M. Domaneschi, DICA, Politecnico di Milano
marco.domaneschi@polimi.it
A. Ghisi, DICA, Politecnico di Milano
aldo.ghisi@polimi.it
S. Griffini, Studio Griffini S.r.l., Milano
stefano.griffini@studiogriffini.eu
G. Novati, DICA, Politecnico di Milano
giorgio.novati@polimi.it
U. Perego, DICA, Politecnico di Milano
umberto.perego@polimi.it
L. Petrini, DICA, Politecnico di Milano
lorenza.petrini@polimi.it
P. Valgoi, A2A, Milano
paolo.valgoi@a2a.eu

SUMMARY – A new version of the Italian design code for dams has been recently introduced, thus replacing after 30 years the previous code, which was still based on a permissible stress design philosophy. The new code follows a limit state approach, employs independent load and resistance factors and defines the earthquake actions in accordance with the new seismic classification of the Italian territory. It assigns at each point of the country its own specific uniform hazard spectrum.
Focusing on the stress verifications of existing large concrete dams, in this paper some of the innovative aspects contained in the new dam code are discussed. Reference is made to two case studies concerning an arch-gravity and a buttress-gravity dam, pointing out the main differences between the current and the previous version of the above-mentioned standards.

Key words: existing concrete dams, stress verifications, seismic forces, finite element method, structural codes, stress limits.

1. Introduction

In Italy the hydroelectric power production in 2013 totaled about 54 GWh, accounting for about 20% of the national electricity production. As in other European countries, in Italy the opportunity to design and build new dams is limited, while there is a strong need to ensure the safety of existing dams. In fact, a service life which often exceeds 5/6 decades may determine structural deterioration.

Existing dams are monitored through appropriate monitoring systems [Bukenya *et al.*, 2014; Chen, 2015], which over the years have evolved substantially from manual mode to a current high level of automation. These systems, supplemented by periodic inspections, allow to promptly identify any abnormal behavior of the dam which then needs to be interpreted to determine its causes. Such structural condition screening activities, nowadays synergetically integrated with the use of numerical simulation tools, belong to the broad area of Structural Health Monitoring (SHM) [Farrar *et al.*, 2007].

Under the standard in-service external actions, the comparison between the actual

response of the dam (in terms of the monitored quantities) and the corresponding results obtained from a FE analysis of the structural model allows to validate the adopted model. Such FE model can then be used to predict structural responses under different static external actions and for quasi-static seismic analyses as well. This procedure is adopted in various studies published in the literature, see for example [Mirzabozorg *et al.*, 2014a], where a double curvature arch dam model is initially validated in order to be subsequently used in further safety analyses.

In this paper two case studies relevant to an existing arch-gravity dam and a buttress dam are presented, focusing on the stress verifications and discussing conceptual and operative differences between the current [DM June 26, 2014] and the previous [DM June 26, 2014] structural code for dams. The comparison between the two codes is the main goal of the present work.

Within this context, the permissible stress method from the previous code is replaced by a limit state approach of the new standard. This development has essential effects in the definition of the loads and the stress verifications. It is herein highlighted by suitable case studies. The overcoming of the permissible stress method refers to the adjustment of the European countries regulatory owing to the introduction of the limit state approach by the international Eurocodes [EN1990-1999].

Furthermore, a new approach for describing Italian seismicity has been introduced. From a subdivision of the territory in large zones having high, medium, low or null seismicity, described by a conventional spectrum, the new code defines the seismic action point by point in terms of parameters defining the specific uniform hazard spectrum. Since both the studied dams are located in the same area in Northern Italy, they can be consistently considered subjected to the same seismic hazard.

According to DM2014, seismic stress verification has to be performed at least for one serviceability and one ultimate limit state: in the present case studies, the damage and the collapse limit states, corresponding to a seismic action having return periods of 100 and 1946 years respectively, have been considered. They are indicated in this work by the Italian acronyms SLD and SLC, respectively.

The generation of the FE models of the existing dams has been carried out starting from the original construction drawings and taking into account the material properties identified by appropriate in-situ tests on the dam concrete and the foundation rock.
The validation of these models, detailed in [Colombo *et al.*, 2016], is performed on the basis of the monitored structural response under in-service conditions.

The stress verifications of an arch-gravity dam and a buttress gravity dam are reported in the following two sections by taking into account seasonal loads (thermal and hydrostatic), modal analysis, and quasi-static seismic actions.

2 Arch-gravity dam

First a large concrete, arch-gravity dam, whose maximum height H is about 130 meters, maximum base thickness t about 20 meters (Figure 1) and crest-arch development about 200 meters, is considered.

The planar dimensions for the rock foundation included in the model are about 900 x 900 meters. Moreover, the rock foundation itself develops about 280 meters farther below the pulvino. These foundation dimensions have been chosen accordingly with parametric studies indicating that a further increase would not modify the response in the region of interest [USACE EM1110-2-6051, 2003]. Figure 2 shows the solid and the finite element models adopted for the dam and the rock foundation.

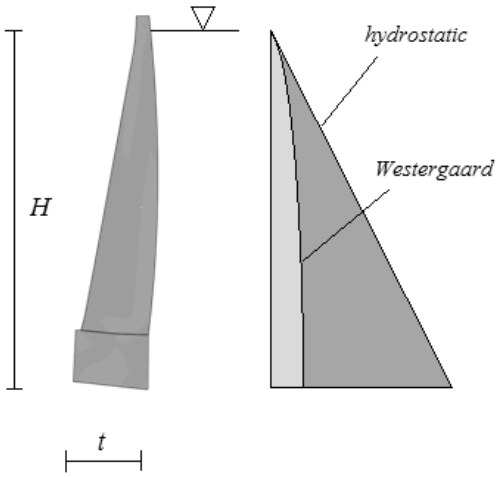

Figure 1 *Crown cross-section of the considered arch-gravity dam, with hydrostatic and Westergaard pressure distributions (maximum level reservoir, SLC)*

In the stress analyses the rock foundation base is fixed, while the lateral surfaces are free, i.e. not restrained at all [Legér *et al.*, 1989].

For this dam typology a pseudo-static analysis with a nonlinear finite element model is adopted, under some assumptions. Two nonlinear artificial joints with uni-lateral contact and friction have been included: the first, at the interface between the dam body and the pulvino, the second one at the interface between the pulvino base and the upper surface of the rock foundation. The first joint models a relevant design feature which is present in many Italian dams. The second one is introduced to account for the no-tension rock foundation behavior: a discontinuity surface could therefore develop, even more when the natural joints in the rock bulk are considered.

Furthermore, since dam concrete can be affected to stiffness degradation due to extensive micro-cracking during the service life of the structure, it is reasonable to assign to such material an elastic-plastic constitutive law. The Drucker-Prager law is then chosen for this first case-study, including a “cap” in the compression regime. It demonstrates able to provide a greater realism to the calculation, smoothing the tensile peaks and simulating the micro-cracking through plastic deformations.

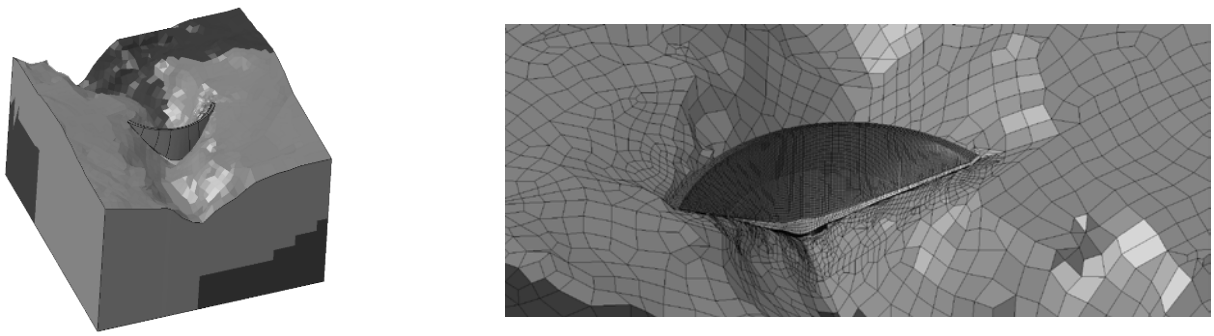

(a) (b)

Figure 2. *Solid (a) and FE model (b) for the considered arch-gravity dam. The rock foundation is also visible*

2.1 *Thermal analysis*

In concrete dams built decades ago, the phenomena of development and dissipation of heat, generated by the hydration reaction of the concrete, are considered completed as well as the shrinkage, with the associated residual stresses. It is instead important to evaluate the stress state induced by temperature changes that occur in the dam due to environmental temperature variations and solar radiation.

The DM2014 requires to consider the effects of thermal actions for any type of dam, while the DM1982 prescribes the evaluation of these effects only for arch dams, for which thermal stresses are typically more significant.

In order to evaluate the thermal strains, $\varepsilon_{ii}^{term}=\alpha\Delta T$ (where the subscript i is associated to the global directions of the reference system, i=1,2,3), to be introduced as input into a structural analysis of the dam, it is first necessary to perform a transient thermal analysis from which the temperature field that develops inside the structure is obtained.

In the literature various contributions, which exemplify and discuss the different types of boundary conditions that can be applied on faces which define the solid under thermal analysis, are available (temperature conditions imposed, convective and radiation type) [Mirzabozorg *et al.*, 2014b]. Typically the temperature on the upstream wet portion is assumed equal to that estimated for the reservoir water, variable in depth. Convection and radiation conditions are imposed on the upstream and downstream free portions, using monitoring data about air temperature and information concerning the sun exposure of the faces in the different seasons.

An advantageous, simplified description of the thermal boundary conditions is possible when a sufficient number of thermometers (embedded in concrete) are present just below the upstream and downstream faces of the dam. In this case, temperature can be assumed as known along the bounding surface of the dam body.

Besides the seasonal variations of the boundary temperature can be considered annually periodic. This hypothesis, assumed as valid for the dam under study, makes it possible to compute, through a thermal transient analysis, a stabilized annual temperature regime $T(\underline{x},t)$ inside the dam; such temperature field is then used to determine the thermal strains to be fed as data into a structural analysis procedure.

More in detail, sinusoidal functions have been used to approximate in time the periodic variation of temperatures on the dam face:

$$T(\underline{x},t) = T_{ref}(\underline{x}) + A(\underline{x})sin(\omega t+\varphi), \tag{2.4}$$

where: $\underline{x}$ is a boundary point; $T(\underline{x},t)$ is the temperature; $T_{ref}(\underline{x})$ is the known average annual temperature at $\underline{x}$; $A(\underline{x})$ is the sinusoidal amplitude at $\underline{x}$; ω is the circular frequency and φ is the phase.

Once the stabilized temperature $T(\underline{x},t)$ has been computed in the dam body, the average annual temperature at interior point $\underline{x}$ is given the role of $T_{ref}(\underline{x})$ and the thermal strains are determined as:

$$\varepsilon_{ii}^{term}(\underline{x},t)= \alpha\,[T(\underline{x},t)-T_{ref}(\underline{x})] =\alpha\,\Delta T(\underline{x},t). \tag{2.5}$$

where: α is the coefficient of thermal expansion.

Figure 5 depicts an example of ΔT time histories relevant to some internal points, showing that the ΔT variation is more marked for external points (e.g. point D) than for internal ones (e.g. B). Furthermore, it turns out that the response at more internal points (like A and B) exhibits a time-delay with respect to more superficial points (e.g. points C and D).

The assumption of annual periodicity of external actions can be regarded as valid also for the hydrostatic load (the monitored data relative to the actual water level variation for the two dams of the present study have confirmed the realism of this assumption). It is thus possible to determine, through an uncoupled thermo-mechanical analysis of the dam, a structural response (in terms of displacements and stresses) which is representative of the typical annual dam behavior under standard in-service conditions. [Colombo *et al.*, 2016].

The most stress-critical situations, relevant to specific times along the year, will be singled out. For such situations, the extra loads represented by the seismic actions will be applied.

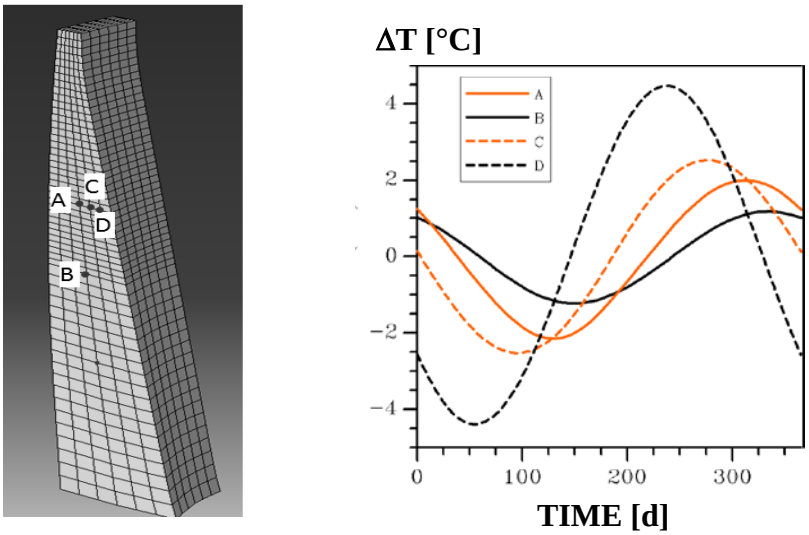

Figure 5. *Time histories of the ΔT at some internal points of the crown cross-section of the dam*

2.2 *Modal analysis*

In order to estimate the components of the seismic forces, it is necessary to compute the natural periods of vibration for the modes which have the largest modal participation mass ratio in the three directions. To this purpose, a modal analysis is carried out using a linear elastic model of the dam-foundation system. Then, the reference seismic accelerations for computing the seismic inertia forces, in all the three directions, are evaluated from the spectra in Figure 4.

Such modal analysis has been conducted for two limit situations: empty reservoir and full reservoir (maximum operating water level). In the latter case “added-masses” have been applied at the nodes of the wet upstream face of the dam. Their value is obtained by considering the Westergaard hydrodynamic overpressures, computing the corresponding FE nodal forces and, finally, dividing such forces by the horizontal peak ground acceleration (a_g=0.063g for SLD, a_g=0.185g for SLC). In the dynamic nodal equilibrium equations the added masses have been associated only to the upstream-downstream direction.

The first ten vibration modes have been computed for the specified two water-level situations (Table 1). In Figure 8 the first four modes are represented (their shape remains qualitatively the same for the two cases of empty and full reservoir). Obviously, with reference to general structural dynamic considerations, increasing the mass due to the presence of the reservoir (maintaining the same stiffness), the vibration periods are larger with respect to the case of empty reservoir.

Table 1. *Frequencies, periods and modal effective masses for the first 10 natural modes: empty and full reservoir. X=upstream-downstream direction, Y=right-left direction, Z=vertical direction.*

	Empty reservoir					**Full reservoir**				
Mode	*f* (Hz)	*T* (s)	Comp. *X* (%)	Comp. *Y*(%)	Comp. *Z* (%)	*f* (Hz)	*T* (s)	Comp. *X* (%)	Comp. *Y*(%)	Comp. *Z* (%)
1	2.85	0.349	38.1	0.5	3.9	1.95	0.511	44.1	0.0	1.3
2	2.95	0.338	1.0	16.2	0.0	2.25	0.443	0.0	6.6	0.0
3	4.06	0.245	13.5	0.0	2.3	3.13	0.318	16.5	0.0	1.2
4	5.04	0.198	0.0	15.5	0.0	3.88	0.257	15.9	0.0	0.1
5	5.56	0.179	13.0	0.0	6.7	4.01	0.249	0.0	5.1	0.0
6	5.84	0.171	0.5	55.2	2.5	4.96	0.201	2.7	0.0	0.1
7	6.07	0.164	11.6	2.4	60.9	5.15	0.194	0.0	4.2	0.0
8	6.32	0.158	0.2	0.1	10.7	5.44	0.183	0.1	69.2	1.5
9	7.16	0.139	0.0	0.9	0.0	5.92	0.168	3.5	1.6	76.1
10	7.60	0.131	0.0	0.1	0.0	6.05	0.165	0.0	0.0	0.1

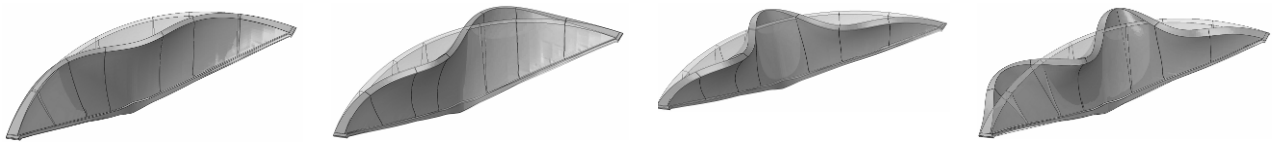

mode 1 mode 2 mode 3 mode 4

Figure 8. *Mode shapes (up to the fourth) for the arch-gravity dam.*

2.3 *Seismic forces*

In the previous national code DM1982 [DM March 24, 1982] the equivalent static seismic forces for the pseudo-static analyses are defined by the seismic level *S* of the area in which dam places. The horizontal and vertical equivalent static forces are evaluated according to the following expressions:

$$F_h = CW\,, \tag{2.1}$$

$$F_v = mCW\,, \tag{2.2}$$

where: *W* is the weight for unit volume of the material [N/m^3]; *m* is a coefficient fixed to 0.5; *C* is the seismic coefficient, equal to

$$C = (S-2)/100\,, \tag{2.3}$$

S is the seismic level (equal to 12, 9 or 6 depending if the zone has high, medium or low seismicity), selected equal to 6 for the present case-study (the site seismicity was considered negligible at the time of construction).

The coefficient *C* allows to define a conventional acceleration response spectrum, which refers to a return period of 475 years and takes into account a reduction factor with respect to an elastic spectrum (equal to 1.5), related to the use of permissible stress method in the analyses, and an additional reduction factor (from 3 to 5), which approximately defines the

structure ductility. This is assumed "*a priori*", independently from the structure typology.

To underline the conventionality of the DM1982 spectrum, it is compared with the elastic spectrum with a period of 475 years obtained for the same site according to DM2014 [DM June 26, 2014]. It is shown (see Figure 3) that to convert DM2014 elastic spectrum into the conventional DM1982 one, first a reduction factor 1.5 is necessary, due to the permissible stress approach. Furthermore, an additional reduction factor of 5 must be applied for structural ductility.

Even though in the DM1982 for arch dams (including the arch-gravity dam here considered) the seismic load, composed by horizontal forces F_h (in the upstream-downstream direction and in cross-stream direction) and the vertical forces F_v must be multiplied by a factor of 2, the difference from the DM2014 loading remains significant.

According to DM2014, one serviceability and one ultimate limit state have to be considered. As anticipated, for the present case-studies, SLD (damage) and SLC (collapse) are adopted. Given the dam geographic coordinates, the corresponding elastic spectra in the horizontal and vertical directions are depicted in Figure 4.

It is worth noting that DM2014 allows to use a design spectrum derived from the elastic one reduced by a ductility factor. However, the choice of a suitable reduction factor would require sophisticated analyses, that rarely are available.

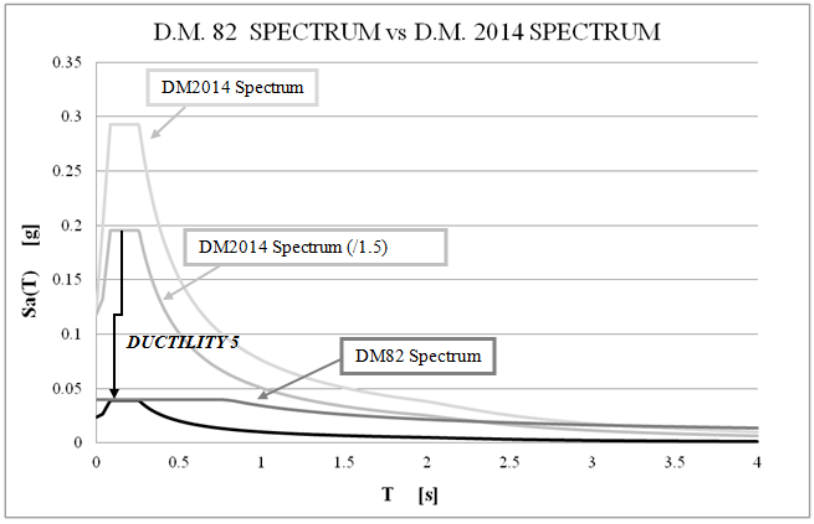

Figure 3. *DM1982 vs DM2014 spectrum, with a further reduction of a factor 1.5 [DM2014 Spectrum(/1.5)] due to permissible stress approach and a factor of 5 due to ductility*

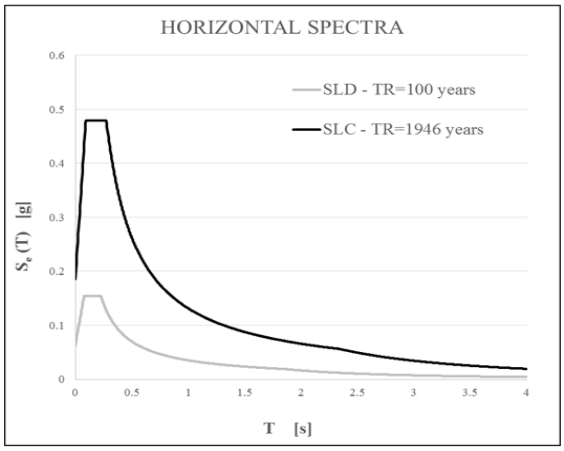

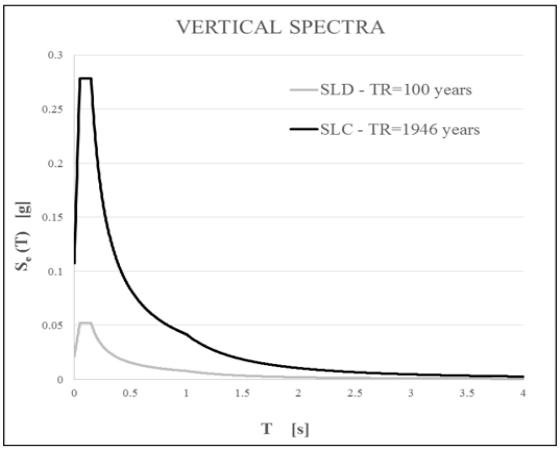

Figure 4. (*Left) horizontal and (right) vertical elastic spectra with 5% damping and a return period of 100 and 1946 years according to DM2014*

2.4 *Other loads*

It is known that in arch dams the determination of the stresses due to self-weight requires the adoption of a "*staged construction*" procedure, in order to take into account (although in an approximate fashion) the geometry changes (and consequent stiffness changes) which occur during dam erection (see e.g. [Pourbakhshian *et al.*, 2015]).

A simplified staged analysis consists in simulating the construction process by fictitious horizontal layers (see Figure 6), carrying out a sequence of corresponding computational steps through which the additional stiffness and self-weight of each new layer is accounted for. The resulting stress field is very different from the one that would be obtained by applying the self-weight in a single analysis referred to the complete dam. If the latter procedure was employed, completely unrealistic tensile stresses would appear near upper portions of the interface between dam body and adjacent rock.

The simplified layer-wise approach provides a stress response which can be considered realistic enough to be used as initial stress state in the analyses accounting for subsequent external actions.

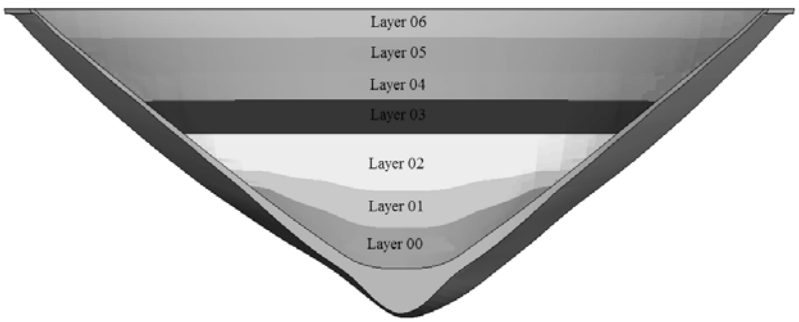

Figure 6. *Subdivision of dam body into layers for the self-weight application*

As for the definition of the hydrostatic load, the available monitored data relevant to reservoir water level over many years, lead to define a typical annual variation for the water level (bold line in Figure 7) for the arch dam under study.

In the analyses the following loading contributions are neglected:

- the rock foundation self-weight, since its effects are pre-existent to the dam construction and they do not influence its response, as long as the rock behaviour is linear elastic [Legér et al., 1989];
- the silt pressure against the dam, since silts deposits have been regularly removed;
- the ice load, since it is negligible.

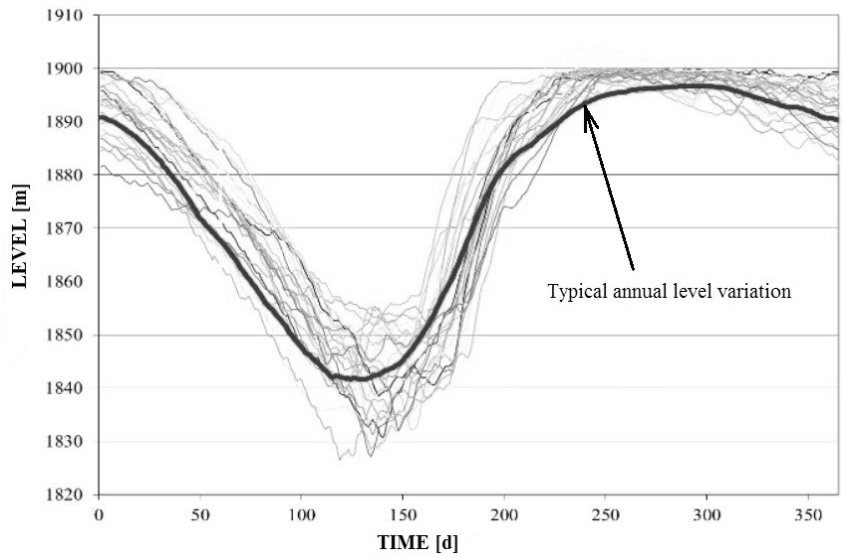

Figure 7. *Average variation of the water level during a typical year*

In the DM2014 for all the concrete dams it is required to calculate the uplift due to the interstitial pressures, while in the DM1982 this load condition is considered for the sliding verification only, therefore it is limited to gravity dams. It is worthwhile to mention that the application of interstitial pressures in a discontinuity surface does not change the total stress state, because of the applied loads [FERC, 2002]. To evaluate the water inertial effects the Westergaard, as described in DM2014 and DM1982, is followed. The most intense (SLC) hydrodynamic overpressure is compared to the hydrostatic pressure in Figure 1.

2.5 *Stress verifications*

DM2014 and DM1982 prescribe similar approaches for structural verifications. They can be summarized into two groups: stress verifications and sliding stability verifications. This article focuses just on the stress verifications.

The verifications are carried out, at all structure points, according to the maximum and minimum principal stresses obtained from FE analysis.

The DM1982, within the permissible stresses approach, prescribes restrictions to maximum stresses (tensile), which are conventional, not related to the actual tensile strength of concrete. Characteristic compression strength derived from experimental measures is adopted for minimum stresses.

According to DM2014, *design* stress verifications at all nodes consist in the comparison of stress resistance R_d to the stresses E_d, resulting from applied actions, for the considered limit state:

$$E_d \leq R_d \tag{2.6}$$

The seismic actions combination for SLC and SLD stress verifications is the following:

$$E + G_1 + G_2 + \psi_{21} \cdot Q_{k1} + \psi_{22} \cdot Q_{k2} + ... \tag{2.7}$$

where E represents the seismic actions; G_1 the permanent forces, i.e. the weight of the dam and the hydrostatic pressure; G_2 the permanent weights of relevant structural elements; Q_{kj}

variable forces (i.e. thermal loads and ice pressure); ψ_{kj} combination coefficients for variable forces (e.g. 0.5 for thermal loads).

For the strength definition the DM2014 refers to the concrete mean mechanical properties, as assessed from mechanical tests. The tensile stress mean value f_{ctm} is assumed for seismic verification at the SLC, while f_{ctm} /1.2 at the SLD. For compression limits, for the seismic verification of existing dams, it is considered reasonable to assume the compression stress mean value f_{cm} as limit value at SLC, and 0.40÷0.60 f_{cm} at SLD. For gravity-buttress dams this value will be reduced to 0.25 f_{cm}.

The definition of stress limit could be associated to a concrete dynamic resistance, which generally exceeds the tensile static strength. For example in the Swiss regulation [Sécurité des ouvrages of accumulation, 2003], the dynamic strength is amplified by 50% when compared to the static value in seismic conditions. Such approach is also reported in several works of the literature, representing an open discussion theme [Raphael, 1984]. It is noted as such strength amplification approach is not mentioned in the DM2014, neither in the DM1982.

For the present case-study, since a nonlinear FE model has been adopted, the actual sequence in which loads have been applied needs to be specified. The following three loading steps have been used:

- step 1: application of self-weight by a staged construction procedure. The goal is the generation of a stress state to be used as “initial stress” in the successive load step;
- step 2: simultaneous application of the hydrostatic load (corresponding to the appropriate reservoir level) and of the thermal load (i.e. of thermal, inelastic strains associated to temperature variations ΔT), both these annually periodic external actions being dependent on the specific time along the year at which the analysis is referred;
- step 3: application of the horizontal ($\pm F_{hx}$, $\pm F_{hy}$) and vertical ($\pm F_{vz}$) seismic forces, together with the hydrodynamic pressure on the wet face of the dam, the latter being considered as a horizontal action in the upstream-downstream direction to be added in the same sense of the corresponding seismic force F_{hx}. The total inertial seismic force for the dam can be estimated by considering the total concrete mass (1.24 10^9 kg) and the added masses associated to the hydrodynamic overpressure (1.3 10^9 kg).

The seismic action is defined in DM2014 by three orthogonal components with appropriate concomitant multiplicative coefficients (differently from the DM1982), which reduce by a factor equal to 0.3 the intensity of seismic action in two main directions. The new code, for nonlinear analyses, allows to consider only one of the two main horizontal seismic components associated to the vertical one.

The signs of these seismic forces are arbitrary, therefore it is necessary to consider the most unfavourable combinations of such forces. For example, the upward direction of the vertical earthquake component usually generate a lightening effect with a non-negligible role. Furthermore, a downwards directed vertical component could be critical for maximum compression stresses. Another critical condition, for arch dams, consists in equivalent static forces acting in downstream-upstream direction.

Following DM1982, the 10 seismic load combinations listed in Table 2 have been considered. Accordingly with DM2014, 30 analyses which have been carried out: half of them are devoted to SLC conditions, the remaining ones to SLD (Table 3 summarizes the SLC cases only).

For both codes the following loads (beside the self-weight of the dam) have been combined with the seismic forces:

- maximum operating water level and two thermal loads, denoted by ΔT_2 and ΔT_3, relevant to two situations which occur during September and January, respectively;
- minimum operating water level, typically occurring in May, and the associated

thermal load denoted by ΔT_1;

- empty reservoir (such condition being interpreted as an exceptional situation caused by a rapid drawdown).

Table 2. *Arch-gravity dam: coefficients for DM1982 seismic load combination*

Analysis	Reservoir	Hydrostatic load	Thermal load	Westergaard overpressure	Seismic Forces		
					F_{hx} (+ upstream-downstream)	F_{hy} (+ right-left)	F_{vz} (+ bottom-up)
Case 01	Min level	1	ΔT_1	0	-2	2	1
Case 02	Min level	1	ΔT_1	1	2	2	1
Case 03	Max level	1	ΔT_2	0	-2	2	1
Case 04	Max level	1	ΔT_2	1	2	2	1
Case 05	Max level	1	ΔT_3	0	-2	2	1
Case 06	Max level	1	ΔT_3	1	2	2	1
Case 07	Empty	0	ΔT_2	0	-2	2	1
Case 08	Empty	0	ΔT_2	0	2	2	1
Case 09	Empty	0	ΔT_3	0	-2	2	1
Case 10	Empty	0	ΔT_3	0	2	2	1

Table 3. *Arch-gravity dam: coefficients for DM2014 seismic load combination (within SLC conditions, return period =1946 years)*

Analysis	Reservoir	Hydrostatic load	Thermal load	Westergaard overpressure	Seismic Forces		
					E_x (+ upstream-downstream)	E_y (+ right-left)	E_z (+ bottom-up)
Case 01	Max level	1	0.5 ΔT_2	1	1	0	0.3
Case 02	Max level	1	0.5 ΔT_2	0	0	1	0.3
Case 03	Max level	1	0.5 ΔT_2	0	-1	0	0.3
Case 04	Max level	1	0.5 ΔT_3	1	1	0	0.3
Case 05	Max level	1	0.5 ΔT_3	0	0	1	0.3
Case 06	Max level	1	0.5 ΔT_3	0	-1	0	0.3
Case 07	Empty	0	0.5 ΔT_2	0	1	0	0.3
Case 08	Empty	0	0.5 ΔT_2	0	0	1	0.3
Case 09	Empty	0	0.5 ΔT_3	0	-1	0	0.3
Case 10	Empty	0	0.5 ΔT_3	0	1	0	0.3
Case 11	Empty	0	0.5 ΔT_3	0	0	1	0.3
Case 12	Empty	0	0.5 ΔT_3	0	-1	0	0.3
Case 13	Min level	1	0.5 ΔT_1	1	1	0	0.3
Case 14	Min level	1	0.5 ΔT_1	0	0	1	0.3
Case 15	Min level	1	0.5 ΔT_1	0	-1	0	0.3

Therefore, the results of few cases are described to allow a comparison among the two code procedures.

For the DM1982 case 04 (self-weight, full reservoir, ΔT_2, seismic forces and hydrodynamic overpressures), Figure 9 shows the maximum and minimum principal stresses, σ_I and σ_{III}, on the upstream face (Figures 9a and 9b), on the pulvino and on a significant transversal vertical section (Figures 9c and 9d). Such stresses, σ_I and σ_{III}, are in agreement

with the code limits (σ_I<1.12 MPa and $|\sigma_{III}|$<11.8 MPa), as defined previously. Plastic strains are disregarded (due to a magnitude of 10^{-5}).

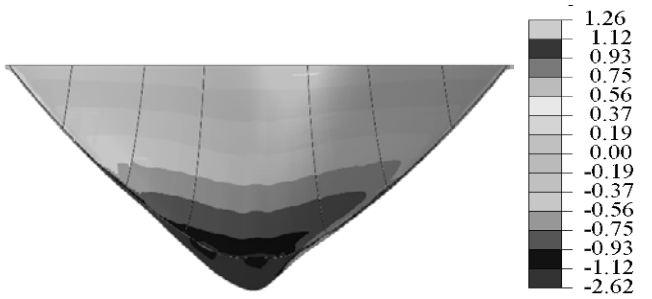

σ in MPa, Max. Principal

(a)

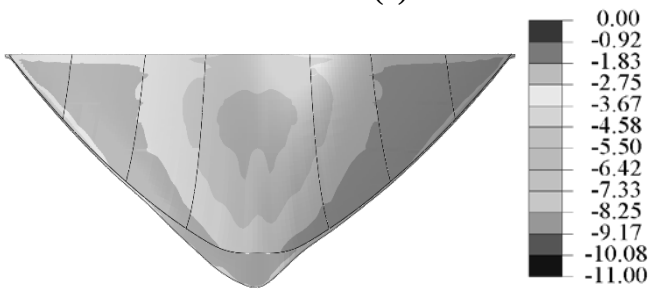

σ in MPa, Min. Principal

(b)

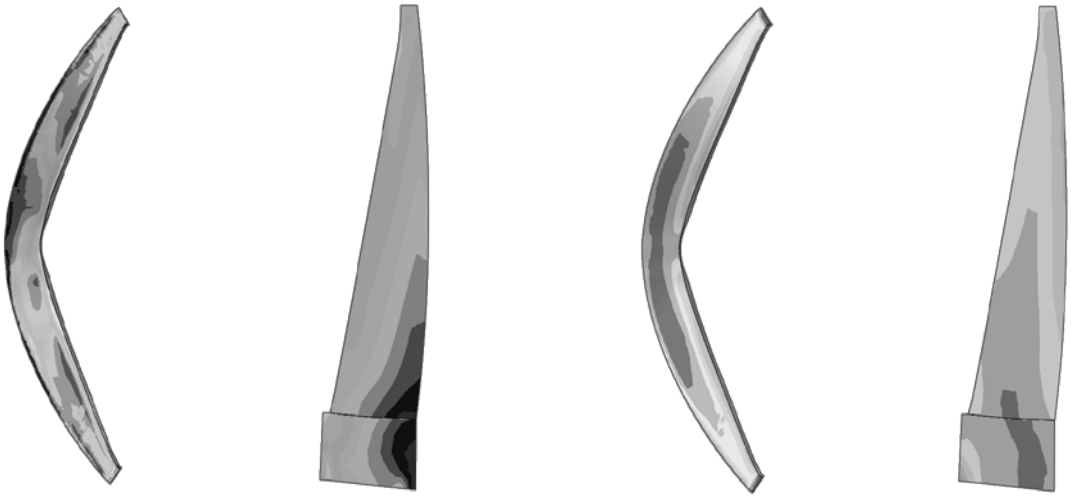

σ in MPa, Max. Principal

(c)

σ in MPa, Min. Principal

(d)

Figure 9. *Principal maximum and minimum stresses for DM1982 case 04. (a-b) upstream face, (c) pulvino and (d) crown cross-section*

For the DM2014 case 01 (self-weight, full reservoir, 0.5 ΔT_2, seismic forces and hydrodynamic overpressures), Figure 10 depicts the maximum and minimum principal stresses, σ_I and σ_{III}, on the upstream face (Figures 10a and 10b), on the pulvino and on a significant transversal vertical section (Figures 10c and 10d). Such stresses, σ_I and σ_{III}, are in agreement with the DM2014 limits (σ_I<2.7 MPa and $|\sigma_{III}|$<49.5 MPa). Plastic strains are disregarded (due to a magnitude of 10^{-5}).

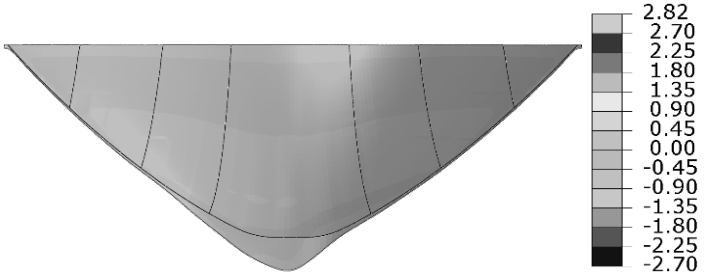

σ in MPa, Max. Principal

(a)

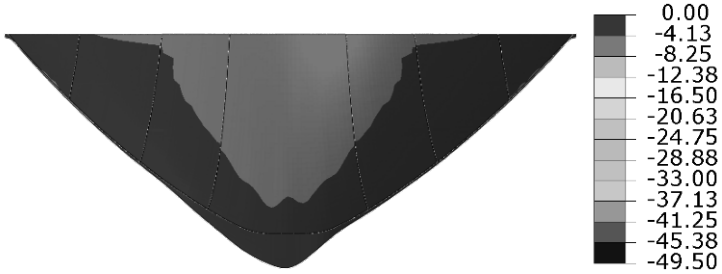

σ in MPa, Min. Principal

(b)

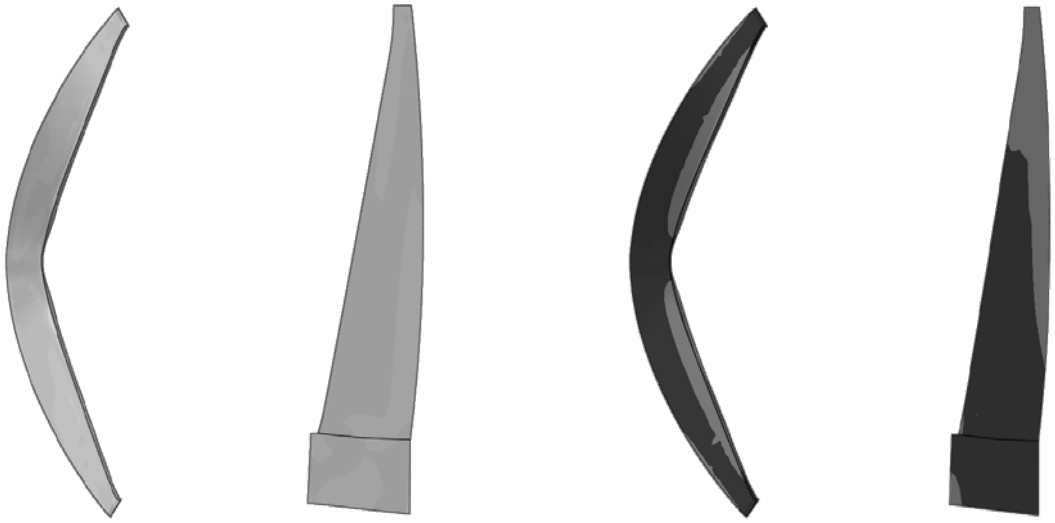

σ in MPa, Max. Principal

(c)

σ in MPa, Min. Principal

(d)

Figure 10. *Principal maximum and minimum stresses for DM2014 SLC case 01. (a-b) upstream face, (c) pulvino and (d) crown cross-section*

Even though for the DM2014 case the seismic actions are one order higher than for the DM1982 code, Figures 9 and 10 highlight how the limit state approach allows higher safety margins with respect to the DM1982. Furthermore, such margins rapidly weaken when the seismic forces act in the opposite arch direction (e.g. from downstream to upstream with empty or minimum reservoir).

3 Buttress gravity dam

As a second application a large concrete buttress gravity dam, about 100 m high and with a crest length of more than 500 m, is considered. The dam is characterized by an upstream reservoir and by a downstream reservoir. It presents a sequence of concrete buttresses. Figure

11 shows the highest one with a total height *H* of 100 m, a base *B* of about 60 m and a thickness *t* of 15 m.

A three-dimensional FE analysis of a central slice of the dam-foundation system, represented in Figure 12, is carried out. Such slice incorporates the two central highest buttresses with the pertinent rock foundation. The lateral surfaces that belong to the planes bounding the considered slice have been constrained in the direction of the lateral abutments and unconstrained in the upstream-downstream and vertical directions. The lower boundary of the rock foundation has been assumed fixed.

For this dam typology, a pseudo-static analysis with a linear finite element model under the following assumptions is proposed. The geometry induces everywhere compression stresses with essential limited zones of concentrations or change of sign, avoiding the need of taking into account joints or nonlinear material properties to have a realistic description of the dam behaviour.

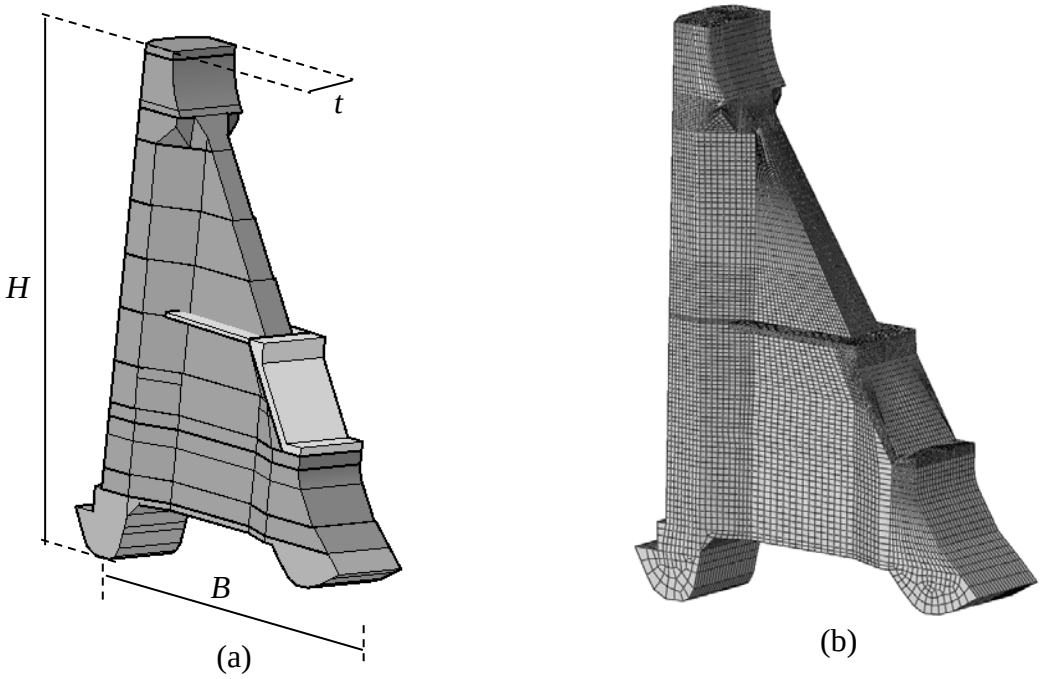

Figure 11. *(a) solid and (b) finite element models of the highest buttress.*

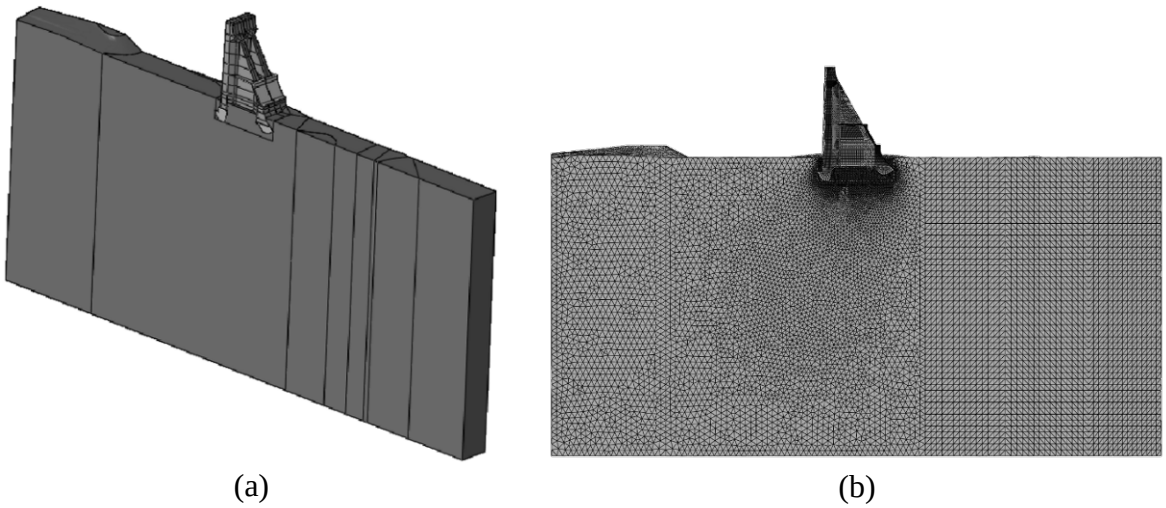

Figure 12. *(a) solid and (b) finite element models of the considered buttress gravity dam*

central module and of the corresponding portion of rock foundation.

3.1 *Thermal analysis*

The procedure performed for evaluating the stabilized annual temperature cycle and the corresponding thermal strains is the same discussed in Section 2.1 for the arch-gravity dam.

3.2 *Modal analysis*

As for the arch-gravity dam case-study, for buttress dams located in seismic regions, DM1982 prescribes that horizontal seismic forces, orthogonal to the buttress middle plane, must be multiplied by two. Despite this prescription, in the case of the considered buttress dam, the effect in terms of stresses of these seismic actions has not been considered in the stress verifications, since it has been verified to be negligible.

The seismic analysis according to the DM2014 is based on the limit state approach, as already discussed for the arch-gravity dam case.

Frequencies, periods and modal masses of the first 6 modes in the cases of empty reservoir and reservoir at maximum operating level are reported in Table 4. First two modes involve a large part of the participating mass in direction X and Z, thus they represent the structural behavior for the horizontal and vertical motions respectively. Consistently with the previous case-study, the modes associated to the maximum reservoir level condition have been computed by using added masses. These masses are the same for the DM1982 and DM2014, as they are independent from soil acceleration.

The first 4 modes are shown in Figure 15. With the exception of the second mode, these are qualitatively the same for the two considered cases of full and empty reservoir.

Table 4. *Natural frequencies, periods and effective modal masses of the first 6 modes for the empty and full reservoir cases. X = downstream direction, Z = vertical direction*

	Empty reservoir				**Full reservoir**			
Mode	*f* (Hz)	*T* (s)	Comp. *X* (%)	Comp. *Z* (%)	*f* (Hz)	*T* (s)	Comp. *X* (%)	Comp. *Z* (%)
1	3.06	0.327	73.5	2.4	2.39	0.418	77.5	1.2
2	5.44	0.184	6.1	91.6	5.26	0.190	11.5	63.3
3	6.62	0.151	18.6	4.9	5.73	0.175	8.0	34.3
4	12.62	0.079	1.6	0.5	11.07	0.090	1.7	0.6
5	14.92	0.067	0.0	0.0	11.87	0.084	0.0	0.0
6	19.90	0.050	0.0	0.3	16.36	0.061	0.0	0.0

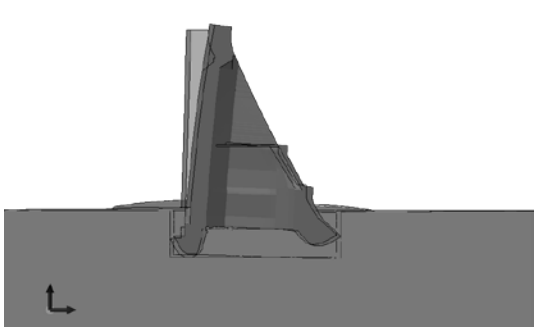

mode 1

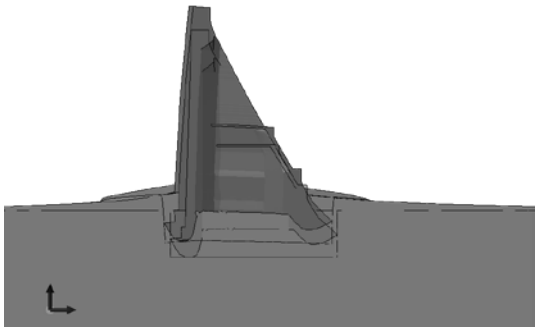

mode 2 (empty reservoir)

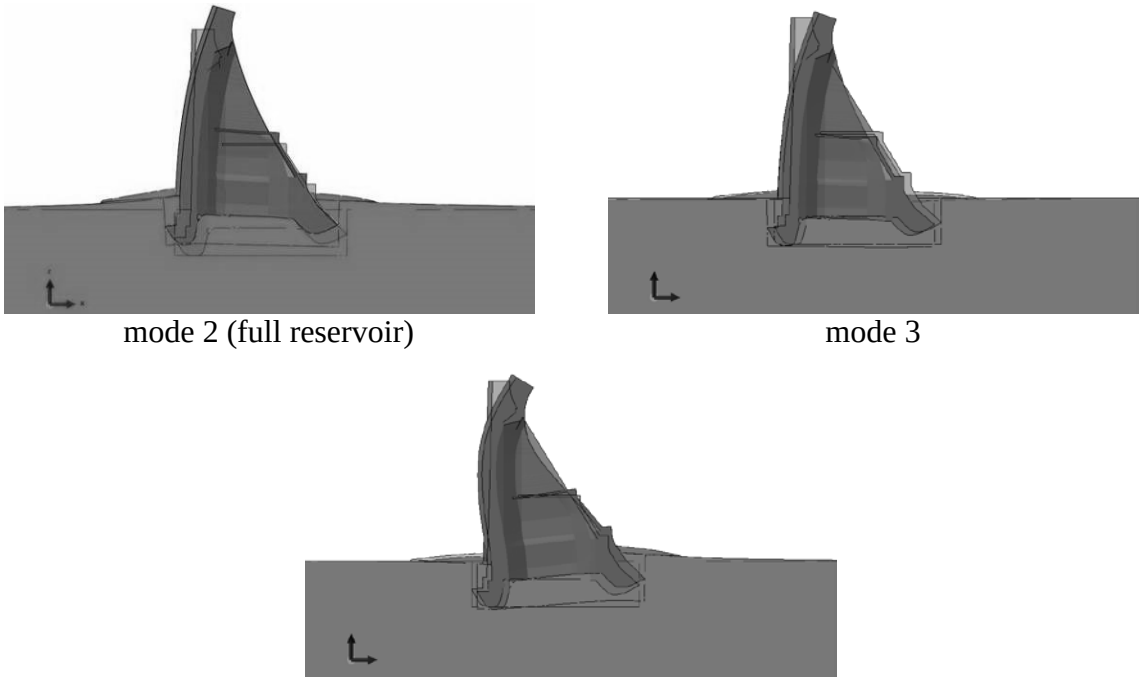

mode 2 (full reservoir) mode 3

mode 4

Figure 15. *First four modes for the buttress gravity dam*

Consistently with the arch-gravity dam case study, the seismic action is defined in DM2014 by three orthogonal components with appropriate concomitant multiplicative coefficients (differently from the DM1982), which reduce by a factor equal to 0.3 the intensity of seismic action in two main directions. Due to the linear approach implemented for the present case-study, which demonstrated appropriate (satisfying the limit stresses assumptions), the dam response to each of the three components E_x, E_y e E_z, has been computed separately and then superposed, according to the expression:

$$1.0 \cdot E_x + 0.3 \cdot E_y + 0.3 \cdot E_z \tag{3.1}$$

considering the possible combinations (including sign change) to single out the most severe effects. As described at the beginning of this section, the E_y component has been neglected.

3.3 *Seismic forces*

Since the dam herein considered is located in the same region of the arch-gravity dam previously dealt with, the considerations of Section 2.3 regarding the definition of the seismic action apply unaltered to study of the arch-gravity dam.

3.4 *Other loads*

In contrast to what discussed for the arch-gravity dam, in the case of buttress-gravity dams the "*staged construction*" procedure does not give rise to significant differences in terms of stress distribution and values compared to the application of the self-weight in a single step, so it has not been adopted.

Since the considered dam is placed between two reservoirs, for the definition of the

hydrostatic load it is necessary to estimate both the upstream and downstream pressures. Only the two conditions of reservoirs empty and full to the highest level have been considered. Figure 13 gives the typical water level annual variation in the reservoirs and allows to associate realistic thermal loads to both the above described reservoir situations.

As in the previous case, the self-weight of the rock mass and of the silting have not been considered. The ice thrust has been accounted for in the stress verifications according to the DM1982 (since ice thickness reaches a value of 0.8 m). It has been neglected in the verifications according to the DM2014, since this type of actions is not considered in the seismic load combination.

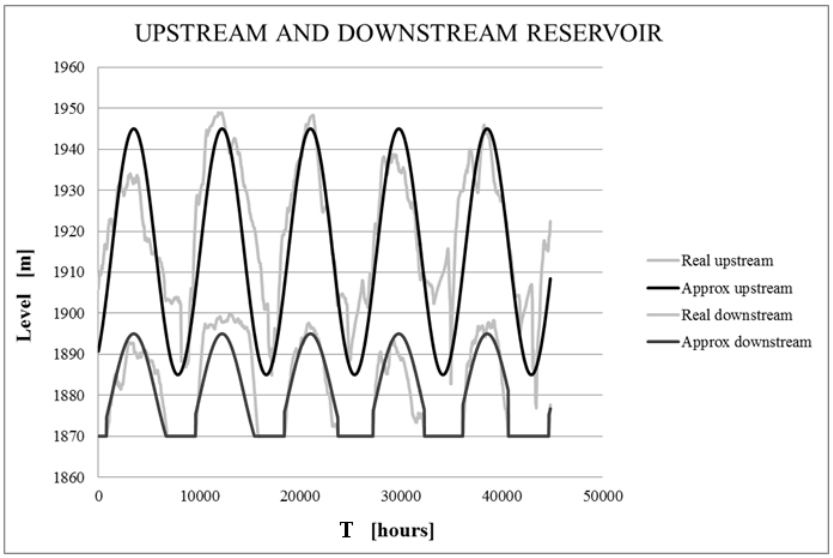

Figure 13. *Monitored upstream and downstream reservoirs level variations and their approximations*

As already mentioned, according to the DM1982, the uplift pressure acting on foundations and construction joints, must be accounted for sliding verifications only. The new code requires to consider such actions also for stress verifications. Figure 14 shows the three-dimensional uplift pressure distribution in the foundation plane on the central dam module. It can be noted the beneficial role played by the internal cavities of the buttress dam in nullifying uplift pressure intensity. This beneficial reduction allows to neglect, for the present case study, the effects in terms of stresses for the final verifications.

About the hydrodynamic overpressure, the same Westergaard approach as described for the arch-gravity dam is used.

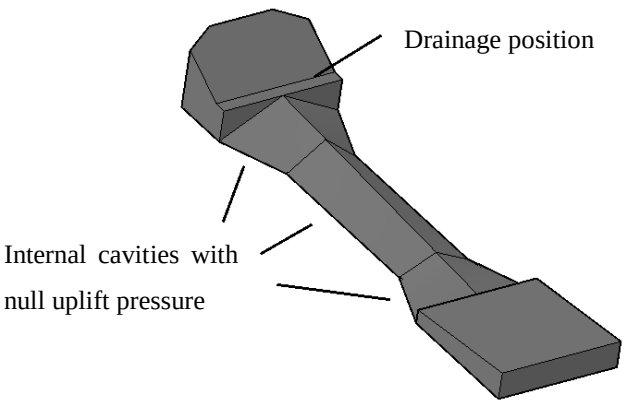

Figure 14. *Three-dimensional view of uplift pressure distribution*

3.5 *Stress verification*

The stress verifications have been carried out for the buttress dam central module, according to the prescriptions for ordinary gravity dams.

According to the DM1982, stresses must be evaluated for the following loading conditions:

- empty reservoir, considering self-weight and seismic actions;
- full reservoir, considering self-weight, downstream and upstream hydrostatic pressure, ice thrust and seismic actions.

According to the DM2014, the stress verification in terms of stresses must be carried out for the following loading conditions:

- empty reservoir, considering self-weight, thermal and seismic actions. Thermal conditions, denoted by ΔT_3, corresponding to January, are used to this purpose;
- full reservoir, considering self-weight, thermal actions, downstream and upstream hydrostatic pressure and seismic actions (with possible uplift pressures). Thermal conditions, denoted by ΔT_1 and ΔT_2, corresponding to September (reservoir maximum level) and April (minimum level), are used.

It can be noted that:

- the total inertial seismic force for the central module of the buttress-gravity dam can be estimated by considering the total concrete mass ($1.69\ 10^8$ kg) and the added masses associated to the hydrodynamic overpressure ($8.4\ 10^7$ kg);
- the thermal action is not considered in the DM1982, whereas it is considered in the DM2014 with a concurrency factor 0.5. For a buttress dam with an irregular geometry and deep joints in the structure thickness, as the one here considered, it is demonstrated (by the authors) that the thermal load plays a significant role. Numerical simulations show that self-stresses due to thermal variations, if considered present with a concurrency factor equal to one, are critical for the strength verification, according to both the DM1982 and DM2014.

For both codes, after computing principal stresses for the different loading conditions, the effects have been superposed and the initial assumption of a linear elastic behavior has been verified.

For the sake of conciseness, the load combinations for the DM1982 and DM2014 are not reported here, since they are equivalent to the same of the arch-gravity dam case, previously discussed.

From stress analyses on the dam structure, the distributions of maximum and minimum principal stresses were obtained. As an example, the results of cases 04 for the DM1982 and 01 for the DM2014 are reported, in Figures 16 and 17 respectively. The reference stress limits have been generally discussed in Section 2.5.

For the case 04 of the DM1982 (self-weight, maximum reservoir, ice, seismic forces and hydrodynamic overpressures), maximum σ_I and minimum σ_{III} principal stresses in the middle section are plotted. Stresses σ_I and σ_{III} respect the limits of the code: uniaxial tensile elastic limit σ_t=0.5 MPa and uniaxial compression elastic limit σ_c=-((R_{ck}-15)/4+6)=-7.75 MPa, assuming R_{ck}=22 MPa on the basis of available laboratory test results.

For case 01 of DM2014 (self-weight, maximum reservoir, 0.5 ΔT_1, seismic forces and hydrodynamic overpressures), the maximum σ_I and minimum σ_{III} principal stresses in the

middle section are plotted in Figure 17. Stresses σ_I and σ_{III} respect the limits of the code (σ_t<2.25 MPa e σ_c>-38 MPa).

From Figures 16 and 17 it is possible to notice that higher limits of the DM2014 allowed larger safety margin, although seismic actions are ten times higher (accordingly to Equation (2.1) for DM1982 and horizontal acceleration spectra in Figure 4 for DM2014) and the thermal action is present with a concurrence coefficient of 0.5.

Furthermore, the superimposition approach herein adopted allowed to compare the contribution of each considered action on the analyzed loading conditions. The role played by the computed thermal effects in the DM2014 stress verifications (disregarded in DM1982) results not negligible with respect to the other actions.

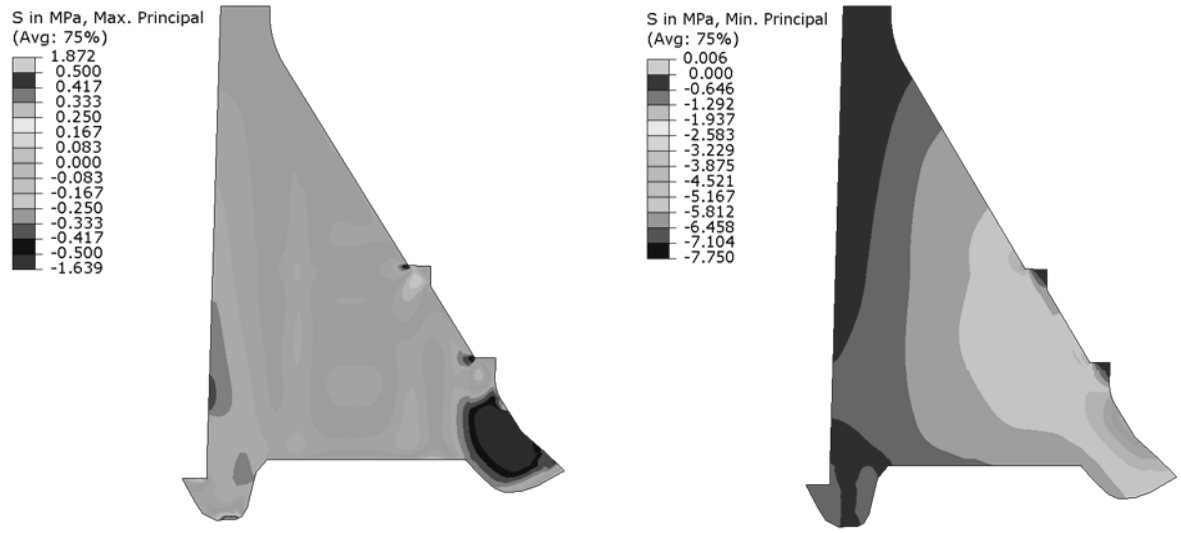

(a) (b)

Figure 16. *(a) maximum and (b) minimum principal stresses for the case 04 of the DM1982. Middle section of the dam central buttress*

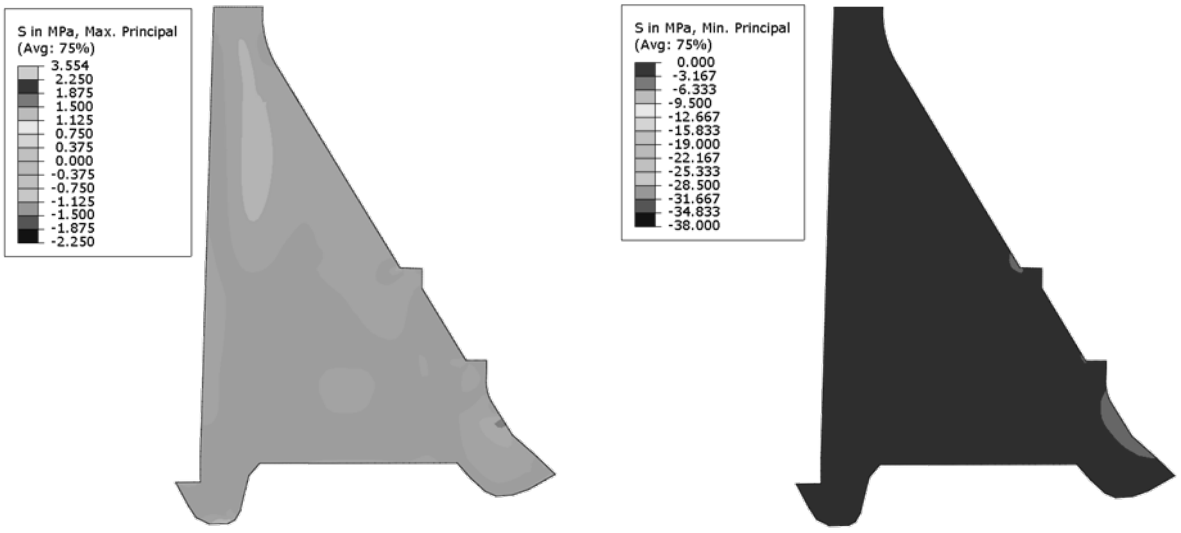

(a) (b)

Figure 17. *(a) maximum and (b) minimum principal stresses for the case 01 of the DM2014 (collapse limit state). Middle section of the dam central buttress*

4. Comments and conclusions

The recent introduction of a new Italian code for design of new dams and the verification of existing ones, based on limit state approach, has motivated the study presented in this paper. The current and the previous codes have been compared focusing on aspects concerning the seismic stress verifications of two existing concrete dams, an arch-gravity and a buttress-gravity dam.

Differences and similarities of the two Italian codes have been discussed with reference to FE analysis procedures and FE models pertinent to the two case studies in point.

Among the various findings that have emerged from the numerical studies conducted, the following results are worth to evidence:

- the new code DM2014 defines the seismic load using different response spectra for each limit state. Overall, these spectra have determined seismic actions more demanding in comparison with the previous code DM1982. On the other side, the new code allows to consider stress limits more realistic and less restrictive in comparison with the ones (markedly conservative) adopted by the permissible stress approach.
- When the arch-gravity dam case-study is considered, the above mentioned safety margins from DM2014 rapidly weaken if the quasi-static seismic forces are conceived as exerted in the upstream direction (with empty reservoir), i.e. in the direction opposite to the one inducing a favorable arch-behavior in the dam.
- The two case studies have confirmed the importance of a fairly accurate preliminary thermal analysis of the dam to determine the thermal strains to fed as data into structural analysis procedures. In fact the thermal stresses have turned out to be as important as those due to the hydrostatic load (maximum level of the reservoir) and to seismic loads.

5. References

Codes:

D.M. 24 March 1982 [1982] *Norme tecniche per la progettazione e la costruzione delle dighe di sbarramento*.

D.M. 26 June 2014 [2014] *Norme tecniche per la progettazione e la costruzione degli sbarramenti di ritenuta (dighe e traverse)*.

EN 1990-1999 [1990-1999] *Eurocodes*. Basis of structural design, 1: Actions on structures, 2: Design of concrete structures, 3: Design of steel structures, 4: Design of composite steel and concrete structures, 5: Design of timber structures, 6: Design of masonry structures, 7: Geotechnical design, 8: Design of structures for earthquake resistance, 9: Design of aluminum structures.

INGV-DPC USACE (US Army Corps of Engineers) EM 1110-2-6051 [2003] *Time-History Dynamic Analysis of Concrete Hydraulic Structures*.

Sécurité des ouvrages d'accumulation [2003] *Documentation de base pour la vérification des ouvrages d'accumulation aux séismes.* Berichte des BWG, SerieWasser - Rapports de l'OFEG, série Eaux 1.2.

FERC [2002] *Engineering Guidelines for the Evaluation of Hydroelectric Projects.*

Journal papers:

Bukenya, P., Moyo, P., Beushausen, H., Oosthuizen, C. [2014] “Health monitoring of concrete dams: a literature review”, *J. Civil Struct Health Monit* **4**, 235–244.
Colombo, M., Domaneschi, M., Ghisi, A. [2016] “Existing concrete dams: loads definition and finite element models validation”, Accepted in *Structural Monitoring and Maintenance*, Techno Press.
Farrar, C. R., Worden, K. [2007] “An Introduction to Structural Health Monitoring”, *Phil. Trans. R. Soc*. A **365**, 303-315.
Ghanaat, Y., and Chudgar, A. K. [2007] “Seismic Design and Evaluation of Concrete Dams – An Engineering Manual”.
Legér, P., and Boughoufalah, M. [1989] “Earthquake input mechanism for time-domain analysis of dam-foundation systems,” *Engineering Structures* **11**, 37–46.
Mirzabozorg, H., Hariri-Ardebili, M.A., Heshmati, M., Seyed-Kolbadi,S.M. [2014a] “Structural safety evaluation of Karun III Dam and calibration of its finite element model using instrumentation and site observation”, *Case Studies in Structural Engineering*, 6–12.
Mirzabozorg, H., Hariri-Ardebili, M.A., Shirkhan, M., Seyed-Kolbadi,S.M. [2014b] “Mathematical Modeling and Numerical Analysis of Thermal Distribution in Arch Dams considering Solar Radiation Effect”, *The Scientific World Journal*, 1-15.
Pourbakhshian, S., Ghaemian, M. [2015] “Investigating Stage Construction in High Concrete Arch Dams”, *Indian Journal of Science and Technology* **8**, No. 14.
Raphael, J. M. [1984] “Tensile Strength of Concrete,” *ACI JOURNAL, Proceedings* **81**, No. 2, 158-165.

Books:
Chen, S.H., “Hydraulics Structures” [2015], Springer-Verlag, Heidelberg, chapter 18.